Supplementary Information

Global softening to manipulate sound velocity for reliable high-performance MgAgSb thermoelectrics

Airan Li[1,†], Longquan Wang[1,2,†], Jiankang Li[1,2], Takao Mori[1,2,*]

[1]*Research Center for Materials Nanoarchitectonics (MANA), National Institute for Materials Science (NIMS), Namiki 1-1, Tsukuba, 305-0044 Japan*

[2]*Graduate School of Pure and Applied Sciences, University of Tsukuba, Tennodai 1-1-1, Tsukuba, 305–8671 Japan*

[*]Email: Mori.Takao@nims.go.jp

[†]These authors contribute equally to this work

Supplementary Notes

Simplified single parabolic band (SPB) model

Based on the SPB model and the assumption of acoustic phonon scattering (APS), the Seebeck coefficient S of materials can be obtained:

$$S = \frac{k_B}{e}\left(\frac{2F_1}{F_0} - \eta\right)$$

$$F_i = \int_0^\infty \frac{\varepsilon^i}{\exp(\varepsilon - \eta) + 1} \mathrm{d}\varepsilon$$

where k_B is the Boltzmann constant, e is the elementary charge, η is the reduced Fermi level, and F_i represents the Fermi integral. From these equations, it is evident that S is determined solely by η of the material, making it a good indicator of η.

In addition to S, the electrical conductivity σ of a material can be expressed as:

$$\sigma = \frac{16\sqrt{2}\pi e^2}{3h^3}\frac{m_d^{*3/2}}{m_I^*}(k_B T)^{3/2}\tau_0 F_0 = \sigma_0 F_0$$

where h is the Planck constant, m_d^* is the density of states effective mass, m_I^* is the inertial effective mass, T is the absolute temperature and τ_0 is the relaxation time. σ_0, named as intrinsic electrical conductivity, includes both the band structure aspect (m_d^* and m_I^*) and carrier scattering aspect (τ_0) of σ.

Because S and F_i are linked to each other through η, F_0 can be expressed in terms of S as follows:

$$F_0 = \exp(2 - S_r) + \frac{\pi^2 / 3S_r}{\exp(2.3S_r)}$$

where $S_r = S/(k_B/e)$ is the reduced Seebeck coefficient. Therefore, σ_0 can be easily obtained from the measured S and σ.

Using the reduced S_r, a simple formula to calculate the Lorenz number L is expressed as:

$$L = (1.47 + \frac{1}{1 + S_r^2}) \times 10^{-8}$$

Moreover, the TE quality factor B can be calculated after obtaining the lattice thermal conductivity κ_L:

$$B = \frac{S_0^2 \sigma_0 T}{\kappa_L}$$

Intrinsic electrical conductivity σ_0 is similar to weighted mobility μ_W and electronic quality factor B_E. Both judge the potential electrical transport performance of the material and are related by the following equation:

$$\sigma_0 = \frac{8\pi e(2m_e k_B T)^{3/2}}{3h^3} \mu_W = B_E / S_0^2$$

where m_e is the mass of the electron and $2S_0 \approx 173$ μV K^{-1}. Therefore, both of them equally describe the electrical transport performance.

Importantly, σ_0 can be further expressed as follows:

$$\sigma_0 = \frac{2\hbar e^2}{3\pi} \frac{N_v}{m_I^*} \frac{C_l}{E_{def}^2}$$

where $\hbar$ N_v, C_l and E_{def} are the reduced Planck constant, band degeneracy, longitudinal

elastic constant and deformation potential, respectively. It is clear that σ_0 is independent of temperature when assuming N_v, m_I^*, C_l and E_{def} are independent of T. Therefore, σ_0 is a good indicator for analyzing the band structure and carrier scattering mechanism, especially considering it can be easily obtained after measuring S and σ.

Debye-Callaway model

Based on the Debye-Callaway model, the lattice thermal conductivity κ_L can be expressed as:

$$\kappa_L = \frac{\kappa_B}{2\pi^2 v}\left(\frac{\kappa_B T}{\hbar}\right)^3 \int_0^{\theta_D/T} \frac{x^4 e^x}{\tau^{-1}\left(e^x - 1\right)^2} dx$$

where $x = \hbar\omega/\kappa_B T$ is the reduced phonon frequency, ω is the phonon frequency, θ_D is the Debye temperature, v is the average phonon group velocity, and τ is the overall phonon scattering relaxation time. Phonon scattering mechanisms, including Umklapp (U) scattering, grain boundary (GB) scattering, nanoparticle (NP) scattering and point defect (PD) scattering are considered in this work. Accordingly, τ can be expressed and simplified as:

$$\tau^{-1} = \tau_{PD}^{-1} + \tau_U^{-1} + \tau_{NP}^{-1} + \tau_{GB}^{-1} = A\omega^4 + B\frac{\omega^2 T}{v^3} + C\frac{\omega^4}{v^3} + \frac{v}{D}$$

where τ_{PD}^{-1}, τ_U^{-1}, τ_{NP}^{-1}, τ_{GB}^{-1} are the phonon relaxation times for PD scattering, U scattering, NP scattering and GB scattering, respectively. The fitting constants A, B, C, D are listed in Table S1.

Supplementary Figures

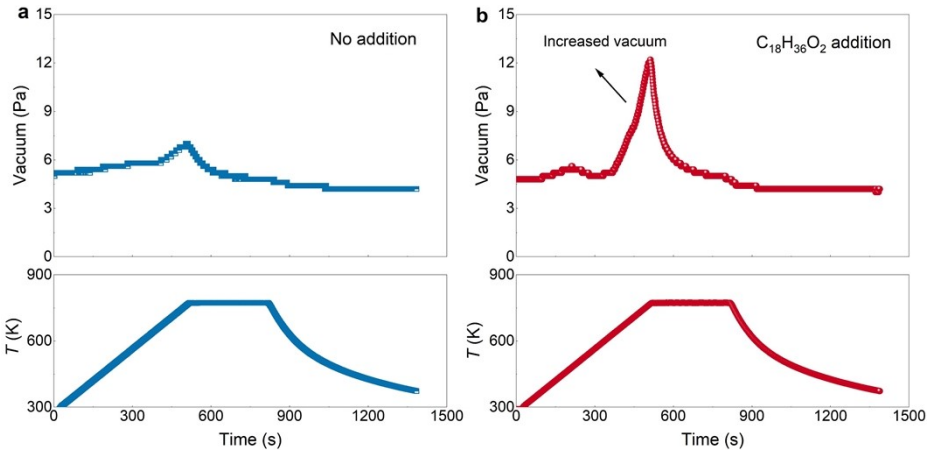

Figure S1. Time dependence of vacuum and temperature *T* for MgAgSb **a** without addition and **b** with 0.75 wt% $C_{18}H_{36}O_2$ addition. The increased vacuum in $C_{18}H_{36}O_2$ addition MgAgSb is due to the decomposition of $C_{18}H_{36}O_2$.

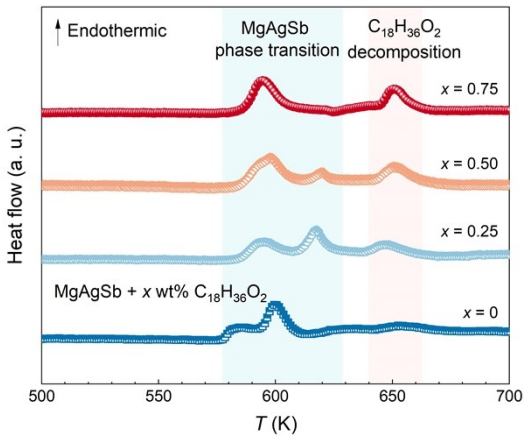

Figure S2. DSC curves of MgAgSb with *x* wt% $C_{18}H_{36}O_2$ addition (*x* = 0, 0.25, 0.5, 0.75). The increased endothermic peaks around 650 K indicate a higher $C_{18}H_{36}O_2$ contents in the samples.

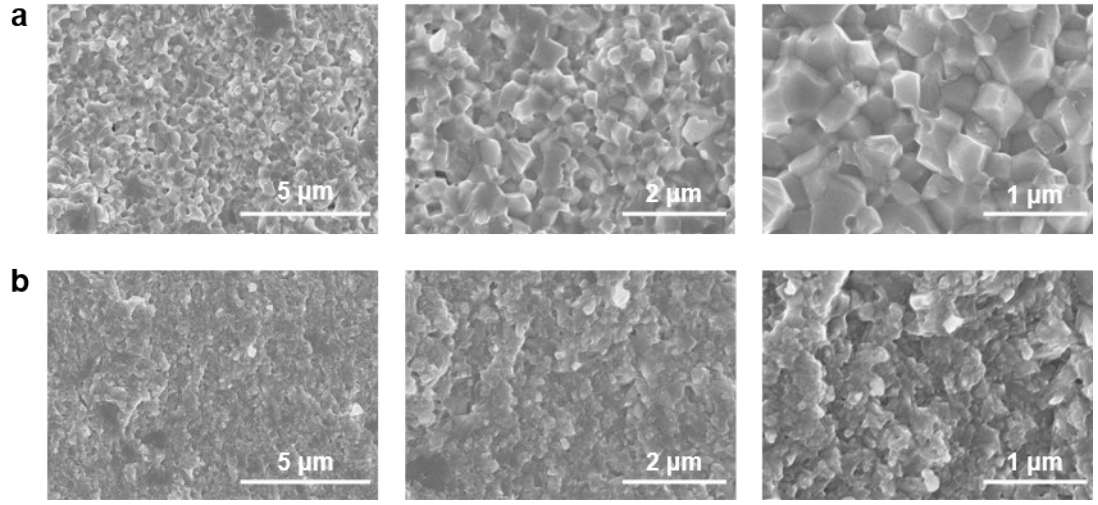

Figure S3 Fracture surface morphology of **a** MgAgSb and **b** MgAgSb with 0.75 wt% stearic acid addition.

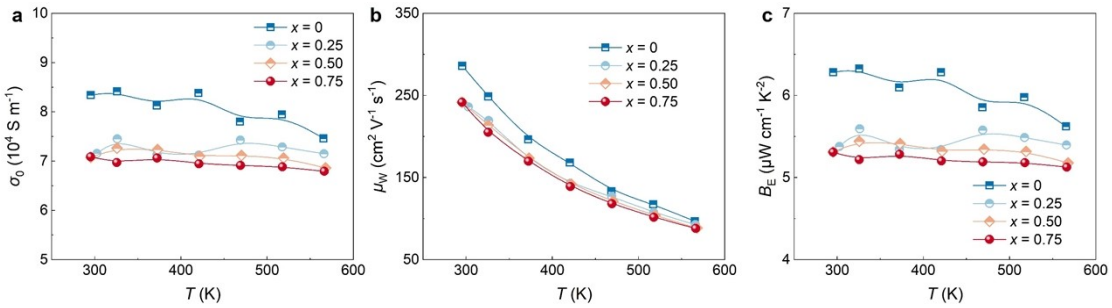

Figure S4. Temperature dependence of **a** intrinsic electrical conductivity σ_0, **b** weighted mobility μ_W and **c** electronic quality factor B_E of MgAgSb with x wt% $C_{18}H_{36}O_2$ addition (x = 0, 0.25, 0.5, 0.75).

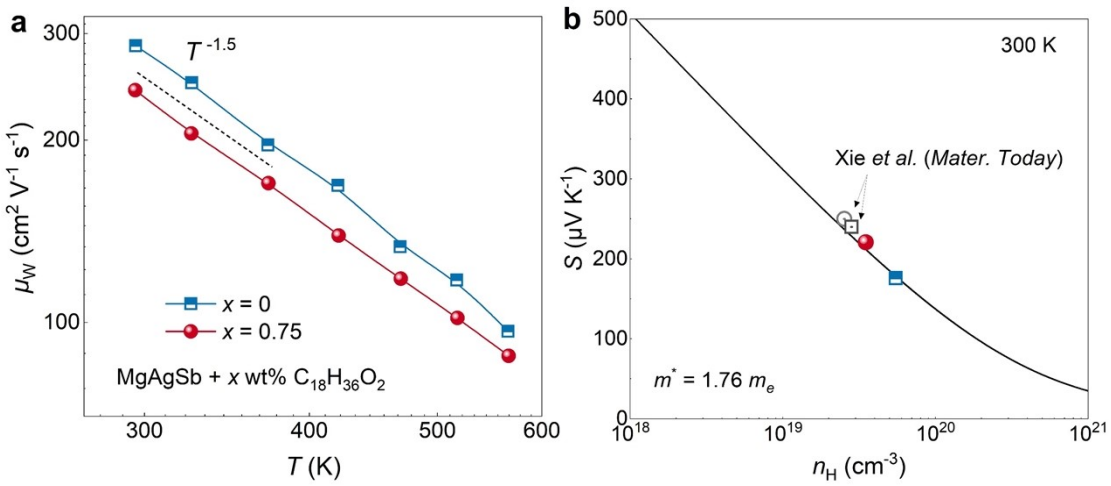

Figure S5 a Temperature dependence of weighted mobility of MgAgSb and MgAgSb with stearic acid addition; **b** the Pisarenko plot of MgAgSb

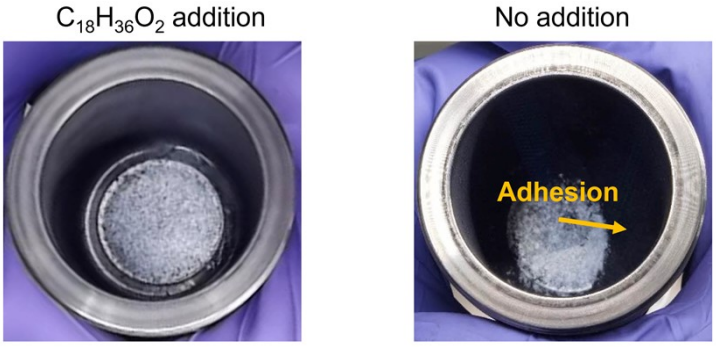

Figure S6. Ball milling jars used in preparing MgAgSb. The MgAgSb with $C_{18}H_{36}O_2$ addition shows minimal powder adhesion to the jar wall, whereas the MgAgSb without addition exhibits serious powder adhesion problem.

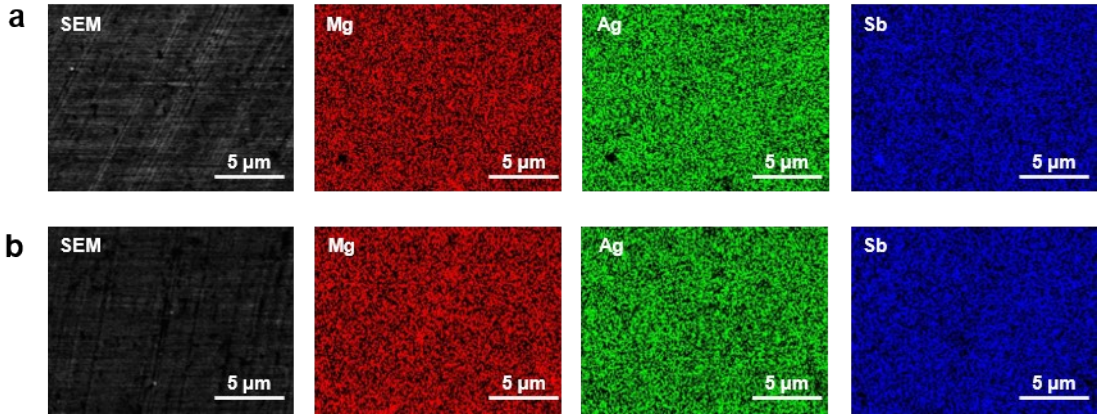

Figure S7 SEM images and elemental EDS mappings of a) MgAgSb and b) MgAgSb with 0.75 wt% stearic acid addition.

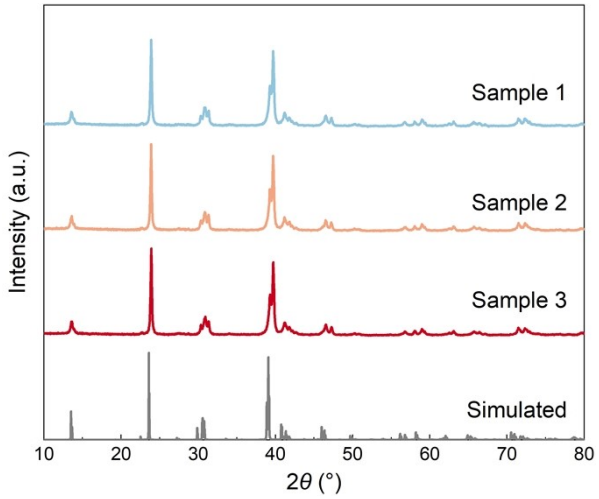

Figure S8. XRD patterns of MgAgSb with 0.75 wt% $C_{18}H_{36}O_2$ addition from three separate syntheses.

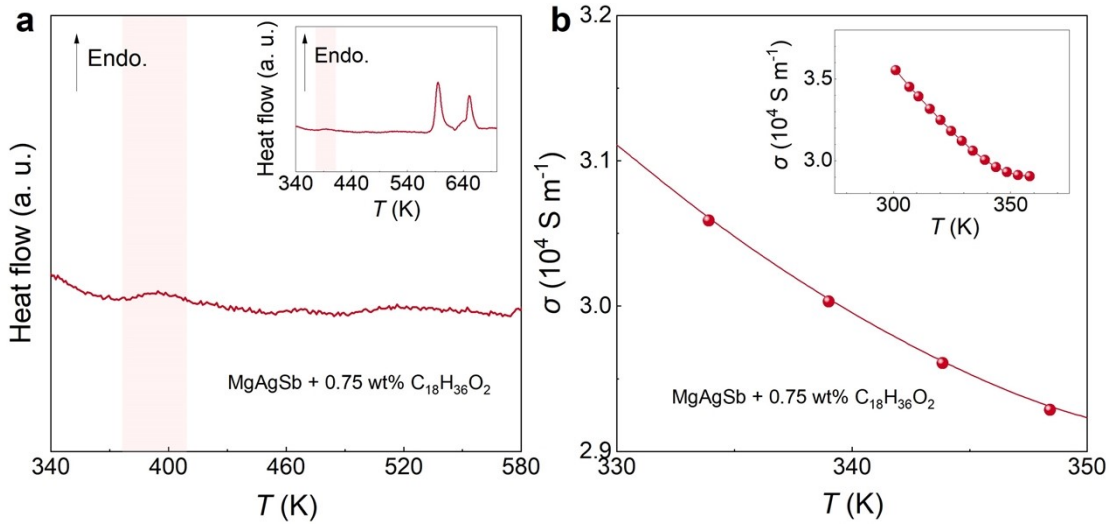

Figure S9 a DSC curve and **b** T dependence of σ of MgAgSb with 0.75 wt% stearic acid addition. The zoomed-out versions of each are shown in the insets.

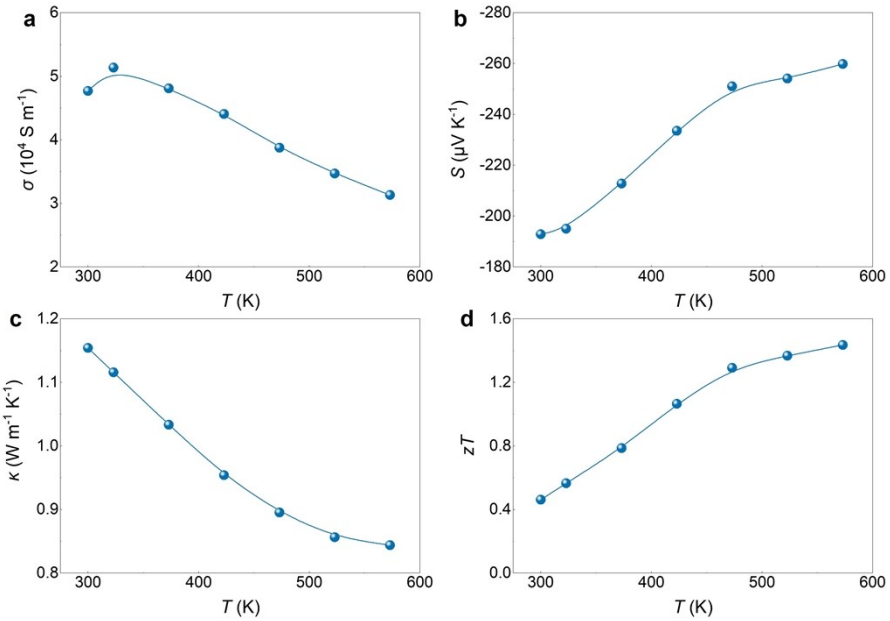

Figure S10. Temperature dependence of **a** electrical conductivity, **b** Seebeck coefficient, **c** thermal conductivity and **d** zT of n-type $Mg_{3.2}In_{0.005}Sb_{1.5}Bi_{0.49}Te_{0.01}$ used in this work

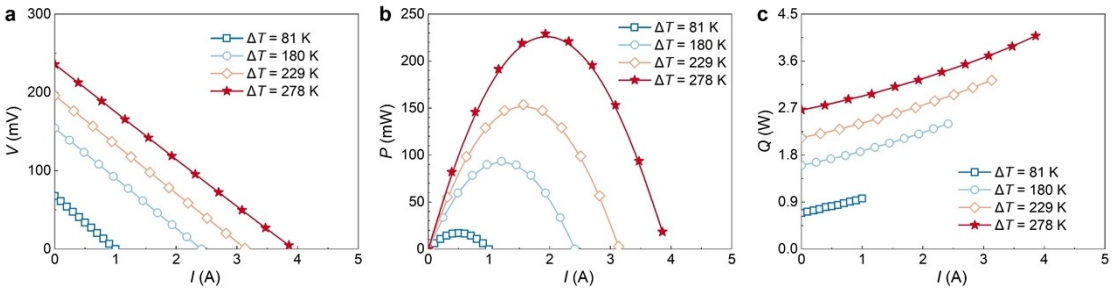

Figure S11. Current *I* dependence of **a** output voltage *V*, **b** output power *P* and **c** heat flow of MgAgSb/$Mg_{3.2}In_{0.005}Sb_{1.5}Bi_{0.49}Te_{0.01}$ two-pair module under different temperature differences.

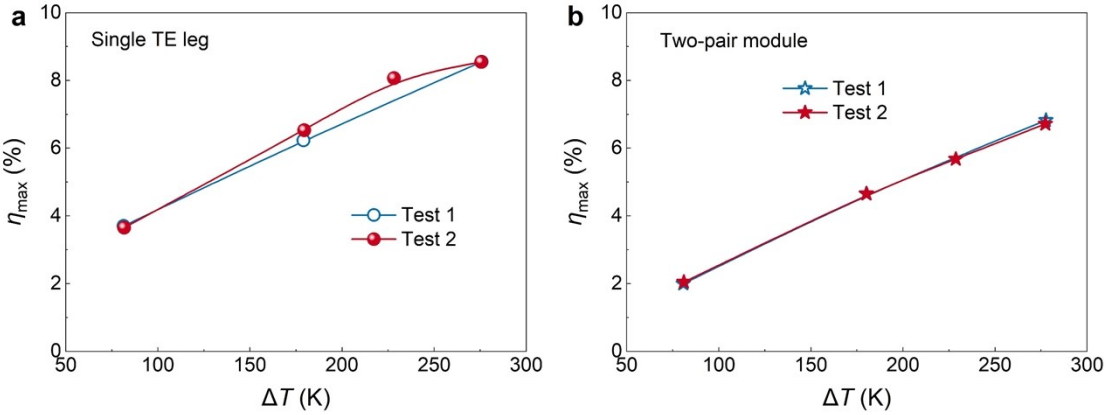

Figure S12. Temperature difference dependence of maximum conversion efficiency of **a** MgAgSb single TE leg and **b** two-pair module in two repeated tests.

Supplementary Table

Table S1. Parameters obtained by fitting the experimental lattice thermal conductivity of MgAgSb using the Debye-Callaway model.

Material	*A*	*B*	*C*	*D*
MgAgSb	3.275e-41	1.2e-07	3.54e-31	5e-7
MgAgSb + 0.75 wt% $C_{18}H_{36}O_2$	3.275e-41	1.2e-07	4.43e-31	2e-7